Letter

Divergence and consensus in majority rule

P. L. Krapivsky
Department of Physics, Boston University, Boston, Massachusetts 02215, USA and Skolkovo Institute of Science and Technology, 143026 Moscow, Russia

S. Redner
Santa Fe Institute, 1399 Hyde Park Road, Santa Fe, New Mexico 87501, USA

(Received 10 March 2021; accepted 1 June 2021; published 15 June 2021)

We investigate majority rule dynamics in a population with two classes of people, each with two opinion states ±1, and with tunable interactions between people in different classes. In an update, a randomly selected group adopts the majority opinion if all group members belong to the same class; if not, majority rule is applied with rate ϵ. Consensus is achieved in a time that scales logarithmically with population size if $\epsilon \geqslant \epsilon_c = \frac{1}{9}$. For $\epsilon < \epsilon_c$, the population can get trapped in a polarized state, with one class preferring the $+1$ state and the other preferring -1. The time to escape this polarized state and reach consensus scales exponentially with population size.

DOI: 10.1103/PhysRevE.103.L060301

A major theme in modeling social dynamics is understanding the conditions that cause a population to either reach consensus or a polarized state, in which a diversity of opinions persists (see, e.g., Refs. [1–4]). The voter model [5–14] provides a simple description for consensus formation. In a single update, a randomly selected voter, which can be in one of two opinion states, adopts the opinion state of a randomly selected neighbor. Consensus is necessarily reached in a finite population. In contrast, polarized states arise in models where interactions between individuals of different classes are limited. Prominent examples include the Axelrod model [15–18], in which individuals interact only if they share a common social trait; the bounded confidence model [19–21], in which individuals interact only if they are sufficiently close in opinion space; multistate voter models, with interactions only between voters in compatible states [22–24]; and social balance models, with edges that specify friendly or unfriendly relations and dynamics that reduce social stress [25–29].

Here, we extend majority rule dynamics [30–38] to probe this tension between consensus and polarization in a mathematically principled way. The original majority rule model describes opinion evolution in a population where each individual can be in one of two equivalent opinion states $+1$ and -1. Individual opinions change as follows: (i) Pick a group of size G (with G odd to ensure that a majority exists) from the population. (ii) All selected individuals adopt the opinion of the group majority. These steps are repeated until the population necessarily reaches consensus, either all $+1$ or all -1. If individuals reside on the nodes of a complete graph, the consensus time scales logarithmically with population size [31]. For finite-dimensional lattices, where the group consists of contiguous individuals, the consensus time scales algebraically with population size [39,40].

Our model, which we term the *homophilous* majority rule (HMR), captures a pervasive aspect of social interactions—namely, homophily [41–43], in that individuals tend to ignore the opinions of people unlike themselves. The simplest situation is a population that consists of two classes of people that we denote as A and B. The update follows that of majority rule, with a simple but crucial twist: (i) Pick a group of individuals at random from the population. (iia) If all group members are from the same class, they adopt the majority opinion. (iib) If the group consists of individuals from different classes, they adopt the majority opinion with rate ϵ; otherwise, no opinion change occurs. Thus the "mixing parameter" ϵ, which we tacitly assume to be less than 1, is the rate at which an individual joins the majority in a heterogeneous group. That is, heterogeneity impedes consensus, a property that has been the focus of considerable social science research (see, e.g., Refs. [44–47]).

When the mixing parameter ϵ exceeds a critical value $\epsilon_c = \frac{1}{9}$, the population quickly reaches consensus, in which the average consensus time scales logarithmically with population size. When $\epsilon < \epsilon_c$, the population can get trapped in a polarized state, with one class preferring the $+1$ state and the other preferring the -1 state. The time to escape this polarized state and reach consensus scales exponentially with population size. For large N, consensus is therefore not achieved in any reasonable timescale. Moreover, the distribution of consensus times contains multiple scales, so that different instances of the population reach consensus at wildly different times.

Rate equations. First, we treat the special case of mixing parameter $\epsilon = 1$ by the deterministic rate equation. We focus on the simplest case of group size $G = 3$ and briefly comment about larger-size groups in the conclusions. The density $\rho(t)$ of individuals with opinion $+1$ evolves according to $\dot{\rho} = \rho^2(1-\rho) - \rho(1-\rho)^2$. The first term accounts for the increase in ρ due to groups that consist of two individuals with opinion $+1$ and one individual with opinion -1. A parallel

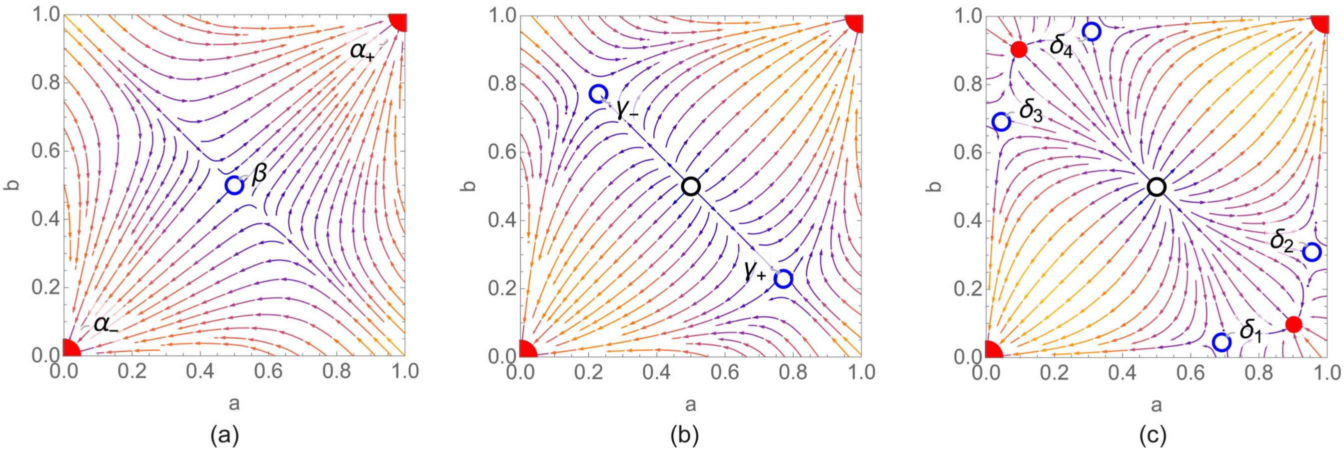

FIG. 1. Flow field of the dynamical system defined by Eq. (1) for the cases: (a) $\epsilon = 0.25$ (greater than $\epsilon^c = \frac{1}{5}$), (b) $\epsilon = 0.15$ (between $\epsilon_c = \frac{1}{9}$ and ϵ^c), and (c) $\epsilon = 0.08$ (less than ϵ_c). The arrow colors indicate the flow magnitude [blue (darker) slow, red (lighter) fast] and the symbols indicate the locations of the fixed points: red dots for stable, blue circles for saddles, and the black circle at $(\frac{1}{2}, \frac{1}{2})$ in (b) and (c) for unstable.

explanation accounts for the second term. The rate equation has two stable fixed points, $\rho = 0, 1$, corresponding to consensus, and an unstable fixed point $\rho = 1/2$. The average consensus time grows logarithmically with system size [31].

Consider now the HMR model for arbitrary $\epsilon \leqslant 1$. We analyze the symmetric situation of $2N$ total individuals, with N in each class. Denote by n_A and n_B the number of A's and B's with opinion state +1. In the $N \to \infty$ limit, the densities $a = n_A/N$ and $b = n_B/N$ obey

$$\dot{a} = F(a) + \epsilon G(a, b), \quad \dot{b} = F(b) + \epsilon G(b, a), \tag{1}$$

where

$$F(x) = x^2(1 - x) - x(1 - x)^2,$$
$$G(x, y) = (1 - x)[2xy + y^2] - x[2(1 - x)(1 - y) + (1 - y)^2]$$

(see the Supplemental Material [48] for details). The dynamical behavior of the system (1) is quite rich, as illustrated by the flow field for generic values of ϵ in each of the three domains: (i) $\epsilon > \epsilon^c = \frac{1}{5}$; (ii) $\epsilon_c < \epsilon < \epsilon^c$ with $\epsilon_c = \frac{1}{9}$; (iii) $\epsilon < \epsilon_c$ (Fig. 1).

When $\epsilon > \epsilon^c$, the consensus fixed points at $\alpha_- \equiv (0, 0)$ and $\alpha_+ \equiv (1, 1)$ are stable nodes, while the fixed point $\beta \equiv (\frac{1}{2}, \frac{1}{2})$ is a saddle. From any initial condition that does not lie on the line $a + b = 1$, the population quickly reaches consensus at α_- for $a + b < 1$ and consensus at α_+ for $a + b > 1$. For initial conditions that lie on the line $a + b = 1$, the population is driven to the fixed point β. However, stochastic finite N fluctuations drive the system from this line (and even from the fixed point β if the evolution begins there) and either consensus is reached with equal probabilities. We show below that the consensus time scales as $\ln N$ in all cases for $\epsilon > \epsilon^c$.

In the intermediate regime, $\epsilon_c < \epsilon < \epsilon^c$, the fixed point β changes from a saddle to an unstable node and two additional saddle-node fixed points

$$\gamma_\pm = \tfrac{1}{2}(1 \pm \Gamma, 1 \mp \Gamma), \quad \Gamma = \sqrt{(1 - 5\epsilon)/(1 - \epsilon)}, \tag{2}$$

emerge from β. These fixed points recede from β as ϵ decreases below ϵ^c while remaining on the line $a + b = 1$ (Fig. 2). According to the rate equations, if the initial condition lies on the line $a + b = 1$, except for $(a, b) = \beta$, the population is drawn to one of the fixed points $\gamma_\pm$. At γ_+, for instance, a fraction $\frac{1}{2}(1 + \Gamma)$ of A's is in the +1 state, while the same majority of B's is in the −1 state. Thus the total population is polarized but evenly balanced, with one-half in the +1 opinion state and the other half in the −1 state. All other initial conditions are again driven to consensus.

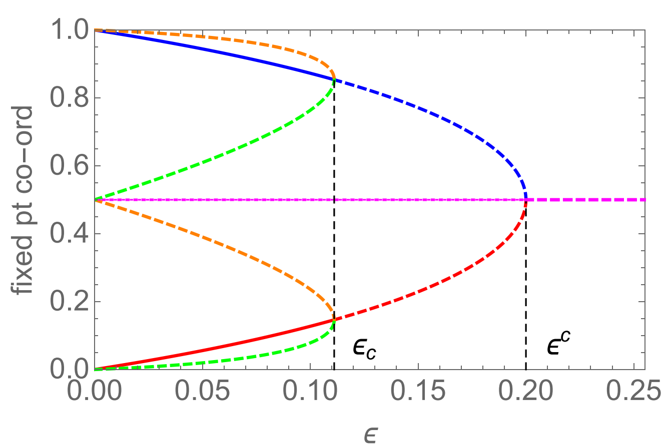

FIG. 2. Fixed-point coordinates as function of ϵ, with dotted, dashed, and solid indicating unstable, saddle, and stable nodes, respectively. Magenta (horizontal line): The symmetric fixed point $\beta = (\frac{1}{2}, \frac{1}{2})$. Red/blue (the parabola that starts at ϵ^c, with the lower branch corresponding to red and the upper branch to blue): The two reflection-symmetric fixed points $\gamma_\pm$ in the range $\epsilon = 0$ to $\epsilon^c = \frac{1}{5}$. For fixed ϵ in this range, the two plotted values give the (x, y) and (y, x) coordinates of $\gamma_\pm$. Green/orange (the two parabolas that start at ϵ_c, with the lower branches corresponding to green and the upper branches to orange): The four nonsymmetric fixed points δ_i that emerge from $\gamma_\pm$ at $\epsilon_c = \frac{1}{9}$. For fixed ϵ, the green (lighter) plotted values give the (y, x) and (x, y) coordinates of δ_1 and δ_3, respectively, while the (darker) orange plotted values give the (x, y) and (y, x) coordinates of δ_2 and δ_4,

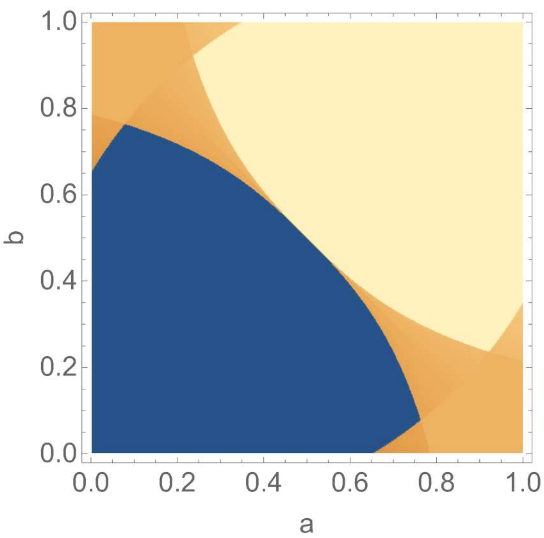

FIG. 3. The basin of attraction to the consensus fixed point (0,0) [blue (black)] and (1,1) [yellow (white)] and to the mixed-opinion fixed points $\gamma_\pm$ [orange (gray)] for the case $\epsilon = 0.1$.

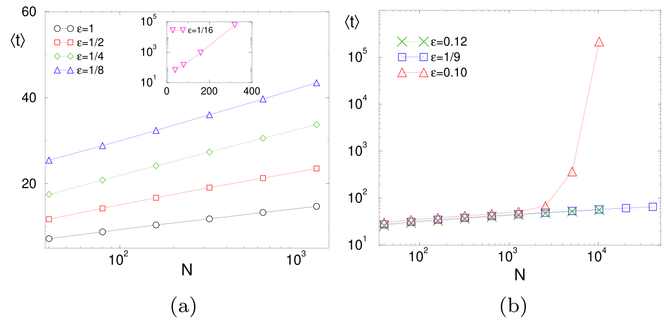

FIG. 4. The average consensus time $\langle t\rangle$ vs N for the balanced initial condition for (a) various ϵ and (b) close to the transition at $\epsilon = \epsilon_c$. In (a), the abscissa is on a logarithmic scale in the main panel and the ordinate is on a logarithmic scale in the inset, where data for the case $\epsilon = \frac{1}{16}$ are shown.

When $\epsilon < \epsilon_c$, four additional fixed points δ_i $(i = 1, 2, 3, 4)$ emerge, two from γ_+ and two from γ_-. These four fixed points are saddle nodes, while the fixed points $\gamma_\pm$ become stable. There are now two disjoint domains in phase space that are attractors to one of these mixed-opinion fixed points $\gamma_\pm$ (Fig. 3). In this regime, the population-average interaction is sufficiently weak that A's and B's form their own and distinct near-consensus enclaves when the initial condition is within either of these basins of attraction for γ_+ or γ_- [Fig. 1(c)]. Again, the population is polarized but evenly balanced and there is a range of initial conditions for which the population is driven to this polarized state. Initial conditions that lie outside these two basins of attraction are again quickly driven to one of the consensus fixed points.

In principle, we can extend the rate equation approach to larger group sizes G, but the analytical calculation quickly becomes intractable. For $G = 5$, a visual inspection of the flow diagram indicates that $\epsilon^c \approx 0.081$ and $\epsilon_c \approx 0.032$, compared to $\epsilon^c = \frac{1}{5}$ and $\epsilon_c = \frac{1}{9}$ for $G = 3$. This decreasing trend suggests that as G increases, ϵ must be extremely small to forestall consensus.

Finite-population simulations. Even for a perfectly mixed population, the rate-equation approach does not fully capture the stochastic dynamics. Because of finite-N fluctuations, the only true attractors of the dynamics are the consensus fixed points. If the population state is in the basin of attraction of one of the fixed points $\gamma_\pm$ (the situation pertinent for $\epsilon < \epsilon_c$), the dynamics first draws the population to one of these fixed points. Eventually, however, a sufficiently large stochastic fluctuation pushes the population out of these basins and to one of the consensus fixed points. The probability to leave either of these basins is exponentially small in N, which implies that the time to reach consensus grows exponentially with N. Although consensus is the true final state, reaching consensus requires a time that is practically unattainable for a population of any appreciable size. Thus for $\epsilon < \epsilon_c$, consensus is effectively not reached.

An analogous dichotomy occurs in population dynamics models, such as the logistic process, where the rate equation predicts a steady state, whereas extinction is the final outcome [49–51]. In these processes, extinction occurs in a time that scales exponentially with the quasisteady-state population size predicted by the rate equation (see, e.g., Refs. [52–55]). The HMR model exhibits a similar rare-event driven approach to a final consensus, but with the additional feature that this approach is governed by two very different timescales.

In our simulations, we first select three individuals at random from the entire population. If these individuals are all from the same class, majority rule is applied. If the group consists of different classes of individuals, majority rule is applied with probability ϵ; otherwise, nothing happens. The time is incremented by $3/N$ in each update so that every individual is considered once, on average, in a single time unit. This update is repeated until consensus is achieved. We investigated several generic initial conditions: (a) a fully polarized state, with A's entirely in the $+1$ state, and B's entirely in the -1 state; (b) a "balanced" state, in which half of both the A's and B's are in the $+1$ state; (c) "imbalanced" states, in which a fraction q of the A's and a fraction $1 - q$ of the B's are in the $+1$ state. This initial condition lies along the line $a + b = 1$ in state space. The results for these initial conditions are qualitatively similar and we primarily focus on the balanced initial condition.

For $\epsilon > \epsilon_c$, the average consensus time $\langle t\rangle$ grows logarithmically with N. This is an exact result [31] for the original MR model ($\epsilon = 1$), and it is also proved to occur for majority-like stochastic processes that are described by rate equations that possess only saddles and sinks—escaping a saddle and reaching a sink takes $O(\ln N)$ time [34,37]. This logarithmic dependence also occurs in the regime $\epsilon_c \leqslant \epsilon \leqslant \epsilon^c$. In this intermediate regime, when the initial state is on the line $a + b = 1$, finite-N fluctuations will drive the population state off this line (where $\gamma_\pm$ are attractors), after which consensus is quickly reached.

When ϵ decreases below $\epsilon_c = \frac{1}{9}$, the N dependence of $\langle t\rangle$ suddenly changes from logarithmic to exponential [Fig. 4(b)]. Strikingly, this exponential dependence sets in only after $N \gtrsim 4000$ for the case $\epsilon = 0.1$, a feature that arises from the geometry of the basin of attraction [Fig. 3(b)]. To reach one

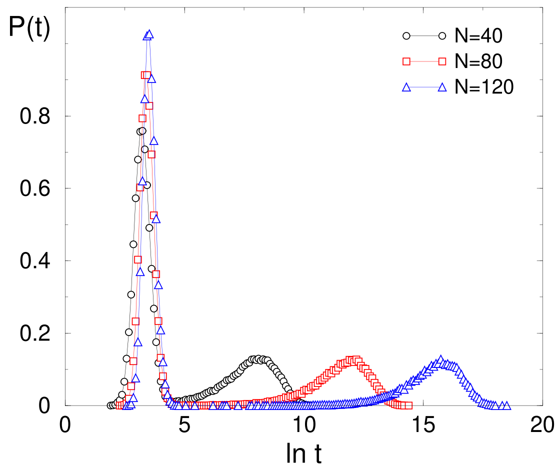

FIG. 5. The consensus-time distribution for the balanced initial condition when $\epsilon = 0.03$ for $N = 40$, 80, and 120.

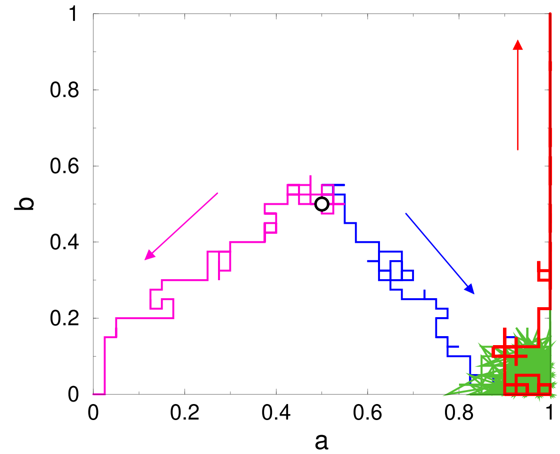

FIG. 6. Two state-space trajectories for $\epsilon = 0.03$ and $N = 80$ that both start from $(\frac{1}{2}, \frac{1}{2})$: (magenta) a trajectory that "directly" goes to consensus at (0,0); (blue/green/red) a "wandering" trajectory that quickly reaches a metastable state near the fixed point γ_+ before eventually reaching consensus.

of the fixed points $\gamma_\pm$ when starting from $(a, b) = (\frac{1}{2}, \frac{1}{2})$, the population state has to navigate within the tongue between the separatrices that border the basins of attraction to $\gamma_\pm$. This tongue is narrow when ϵ is close to ϵ_c, so the population state is typically and quickly drawn to a consensus fixed point in this range. However, if either fixed point $\gamma_\pm$ is reached, the escape time scales exponentially with N. These two outcomes explain the existence of two drastically different timescales in $P(t)$, the consensus-time distribution (Fig. 5). We may estimate the probabilities of the two outcomes from the data for $P(t)$ and find that the probability to reach one of the fixed points $\gamma_\pm$ vanishes as $\epsilon \to \epsilon_c$ from below; a bound for this probability is given in the Supplemental Material. Finally, note that this bimodal consensus-time distribution (Fig. 5) arises when the starting state is $(a, b) = (\frac{1}{2}, \frac{1}{2})$. If the starting point lies inside the basin of attraction of $\gamma_\pm$, the consensus-time distribution is asymptotically exponential, $P(t) = \langle t\rangle^{-1} e^{-t/\langle t\rangle}$, and is fully characterized by the average consensus time [55].

Deep in the ultraslow regime, these two disparate timescales can be readily quantified. For example, for $\epsilon = 0.03$, the average consensus time $\langle t\rangle$ over 10^5 realizations is approximately 1304, 57 104, and 2 477 250 for $N = 40$, 80, and 120. The underlying distribution of consensus times consists of two widely separated peaks (Fig. 5). These peaks are located at roughly $t \approx 23.8$ and 3.3×10^3 for $N = 40$, $t \approx 29$ and 1.6×10^5 for $N = 80$, and $t \approx 33$ and 8.9×10^6 for $N = 120$. The smaller of these two times grows close to logarithmically with N, while the larger time grows roughly exponentially with N. Thus the average consensus time is not a useful measure of how long it takes a given realization of the population to reach consensus.

To appreciate the dynamical source of these disparate timescales for $\epsilon < \epsilon_c$, it is useful to trace individual state-space trajectories. Figure 6 shows two such trajectories for $\epsilon = 0.03$ and $N = 80$. One (magenta) corresponds to quick consensus, in which the trajectory moves quasisystematically from the initial state of $(a, b) = (\frac{1}{2}, \frac{1}{2})$ to consensus at (0,0) in a time of roughly 29.5. The other trajectory (multiple colors) shows an ultraslow approach to consensus. The blue portion shows the first 100 steps, where the population state quickly goes from $(\frac{1}{2}, \frac{1}{2})$ to a metastable state near the fixed point $\gamma_+ \approx (0.968, 0.032)$. The green portion shows the trajectory in the time range between $t \approx 100$ and $0.999T$, where $T = 126\,456$ is the consensus time for this trajectory. This part of the trajectory wanders stochastically about the fixed point γ_+ until a large fluctuation drives this trajectory outside the local basin of attraction, after which the consensus fixed point at (1,1) is reached (red portion of the trajectory).

When $\epsilon = \epsilon_c$, which defines the boundary between logarithmic and exponential dependence of the average consensus time, we might expect $\langle t\rangle$ to scale algebraically with N. Instead, simulations indicate logarithmic scaling [Fig. 4(b)]. We also might anticipate that the consensus time is a non-self-averaging random quantity in the intermediate regime $\epsilon_c \leqslant \epsilon \leqslant \epsilon^c$ because of the presence of the fixed points $\gamma_\pm$. However, simulations suggest that the consensus time is self-averaging for all $\epsilon \geqslant \epsilon_c$. Specifically, we found that the fluctuation measure $R \equiv \sqrt{\langle t^2\rangle}/\langle t\rangle \to 1$ faster than algebraically in N when $\epsilon > \epsilon_c$, and as $N^{-1/2}$ when $\epsilon = \epsilon_c$. These results suggest that the consensus time t is a self-averaging random quantity that scales as $\ln N$ for all $\epsilon \geqslant \epsilon_c$.

Majority rule in a two-class population favors quick consensus (logarithmic in population size N) when individuals heed members of the other class with a rate greater than 11%. Otherwise, a polarized state typically occurs, in which one class favors the +1 opinion and the other class favors −1, even though neither class has an internal opinion preference. This polarized state is practically eternal in that the escape time to reach consensus scales exponentially with N. This frozen-in polarization seems characteristic of the current social climate [56–59] and illustrates the crucial role of interactions between different classes of individuals in fostering either camaraderie or animosity. However, as the group size G increases, there is a wider range of values for the mixing parameter ϵ for which polarization appears to be less likely. Our work also raises several challenges, such as understanding homophilous majority rule on more realistic or dynamically evolving networks, heterogeneous groupings of individuals, and the role of more than two opinion states.

We thank Mirta Galesic and Mauro Mobilia for helpful suggestions. S.R. was partially supported by NSF Grant No. DMR-1910736.

[1] C. Castellano, S. Fortunato, and V. Loreto, Rev. Mod. Phys. **81**, 591 (2009).

[2] S. Galam, *Sociophysics: A Physicist's Modeling of Psycho-political Phenomena* (Springer, Berlin, 2012).

[3] K. Sznajd-Weron and J. Sznajd, Int. J. Mod. Phys. C **11**, 1157 (2000).

[4] M. Galesic and D. L. Stein, Physica A **519**, 275 (2019).

[5] P. Clifford and A. Sudbury, Biometrika **60**, 581 (1973).

[6] R. A. Holley and T. M. Liggett, Ann. Probab. **3**, 643 (1975).

[7] J. T. Cox, Ann. Probab. **17**, 1333 (1989).

[8] T. M. Liggett, *Stochastic Interacting Systems: Contact, Voter and Exclusion Processes*, Vol. 324 (Springer, Berlin, 2013).

[9] P. L. Krapivsky, Phys. Rev. A **45**, 1067 (1992).

[10] L. Frachebourg and P. L. Krapivsky, Phys. Rev. E **53**, R3009(R) (1996).

[11] I. Dornic, H. Chaté, J. Chave, and H. Hinrichsen, Phys. Rev. Lett. **87**, 045701 (2001).

[12] P. L. Krapivsky, S. Redner, and E. Ben-Naim, *A Kinetic View of Statistical Physics* (Cambridge University Press, Cambridge, UK, 2010).

[13] A. Baronchelli, R. Soc. Open Sci. **5**, 172189 (2018).

[14] S. Redner, C. R. Phys. **20**, 275 (2019).

[15] R. Axelrod, J. Conflict Resolut. **41**, 203 (1997).

[16] R. Axtell, R. Axelrod, J. M. Epstein, and M. D. Cohen, Comput. Math. Organ. Theory **1**, 123 (1996).

[17] C. Castellano, M. Marsili, and A. Vespignani, Phys. Rev. Lett. **85**, 3536 (2000).

[18] F. Vázquez and S. Redner, Europhys. Lett. **78**, 18002 (2007).

[19] G. Weisbuch, G. Deffuant, F. Amblard, and J.-P. Nadal, Complexity **7**, 55 (2002).

[20] R. Hegselmann and U. Krause, J. Artif. Soc. Social Simul. **5**, 1 (2002).

[21] E. Ben-Naim, P. L. Krapivsky, and S. Redner, Physica D **183**, 190 (2003).

[22] F. Vazquez, P. L. Krapivsky, and S. Redner, J. Phys. A: Math. Gen. **36**, L61 (2003).

[23] S. A. Marvel, H. Hong, A. Papush, and S. H. Strogatz, Phys. Rev. Lett. **109**, 118702 (2012).

[24] M. Mobilia, Europhys. Lett. **95**, 50002 (2011).

[25] T. Antal, P. L. Krapivsky, and S. Redner, Phys. Rev. E **72**, 036121 (2005).

[26] K. Kułakowski, P. Gawroński, and P. Gronek, Int. J. Mod. Phys. C **16**, 707 (2005).

[27] T. Antal, P. L. Krapivsky, and S. Redner, Physica D **224**, 130 (2006).

[28] S. A. Marvel, J. Kleinberg, R. D. Kleinberg, and S. H. Strogatz, Proc. Natl. Acad. Sci. USA **108**, 1771 (2011).

[29] T. Minh Pham, I. Kondor, R. Hanel, and S. Thurner, J. R. Soc. Interface **17**, 20200752 (2020).

[30] S. Galam, Physica A **274**, 132 (1999).

[31] P. L. Krapivsky and S. Redner, Phys. Rev. Lett. **90**, 238701 (2003).

[32] M. Mobilia and S. Redner, Phys. Rev. E **68**, 046106 (2003).

[33] N. Crokidakis and P. M. C. de Oliveira, Phys. Rev. E **92**, 062122 (2015).

[34] G. Schoenebeck and F.-Y. Yu, in *Proceedings of the Twenty-Ninth Annual ACM-SIAM Symposium on Discrete Algorithms* (SIAM, Philadelphia, 2018), pp. 1945–1964.

[35] A. Mukhopadhyay, R. R. Mazumdar, and R. Roy, J. Stat. Phys. **181**, 1239 (2020).

[36] V. X. Nguyen, G. Xiao, X. J. Xu, Q. Wu, and C.-Y. Xia, Sci. Rep. **10**, 456 (2020).

[37] G. Schoenebeck and F.-Y. Yu, in *Proceedings of the 21st ACM Conference on Economics and Computation* (ACM, New York, 2020), pp. 49–67.

[38] J. Noonan and R. Lambiotte, arXiv:2101.03632.

[39] P. Chen and S. Redner, Phys. Rev. E **71**, 036101 (2005).

[40] P. Chen and S. Redner, J. Phys. A **38**, 7239 (2005).

[41] M. McPherson, L. Smith-Lovin, and J. M. Cook, Ann. Rev. Sociol. **27**, 415 (2001).

[42] G. Kossinets and D. J. Watts, Am. J. Sociol. **115**, 405 (2009).

[43] P. Barberá, Polit. Anal. **23**, 76 (2015).

[44] E. Mannix and M. A. Neale, Psychol. Sci. Public Interest **6**, 31 (2005).

[45] S. W. Kozlowski and D. R. Ilgen, Psychol. Sci. Public Interest **7**, 77 (2006).

[46] B. De Jong, N. Gillespie, I. Williamson, and C. Gill, J. Management (2020), doi: 10.1177/0149206320943658.

[47] L. P. Moyer, J. Szmer, S. Haire, and R. K. Christensen, Politics Groups Identities **8**, 822 (2020).

[48] See Supplemental Material at http://link.aps.org/supplemental/10.1103/PhysRevE.103.L060301 for the details of the rate-equation solution.

[49] S. Karlin and J. McGregor, *Stochastic Models in Medicine and Biology* (University of Wisconsin Press, Madison, WI, 1964).

[50] I. Nåsell, *Extinction and Quasi-stationarity in the Stochastic Logistic SIS Model* (Springer, Berlin, 2011).

[51] J. Allen, *Stochastic Population and Epidemic Models — Persistence and Extinction* (Springer, Berlin, 2015).

[52] V. Elgart and A. Kamenev, Phys. Rev. E **70**, 041106 (2004).

[53] D. A. Kessler and N. M. Shnerb, J. Stat. Phys. **127**, 861 (2007).

[54] M. Assaf and B. Meerson, Phys. Rev. E **81**, 021116 (2010).

[55] M. Assaf and B. Meerson, J. Phys. A **50**, 263001 (2017).

[56] L. A. Adamic and N. Glance, in *Proceedings of the 3rd International Workshop on Link Discovery* (ACM, New York, 2005), pp. 36–43.

[57] Y. Wang, J. Luo, and X. Zhang, in *International Conference on Social Informatics* (Springer, Berlin, 2017), pp. 409–425.

[58] Y. Wang and J. Luo, arXiv:1802.00156.

[59] F. Baumann, P. Lorenz-Spreen, I. M. Sokolov, and M. Starnini, Phys. Rev. X **11**, 011012 (2021).